LASER ABLATION OF CONCRETE*

Michael Savina[1], Zhiyue Xu[2], Yong Wang[2], Michael Pellin[1], and Keng Leong[2]

[1]Argonne National Laboratory
Materials Science and Chemistry Divisions
Argonne, Illinois USA

[2]Argonne National Laboratory
Technology Development Division
Argonne, Illinois USA

Submitted for publication in the

ICALEO'98 Proceedings
Orlando, Florida
November 16-19, 1998

*Work supported by the U.S. Department of Energy, BES-Materials Science, under Contract W-31-109-ENG-38, and by the U.S. Department of Energy, Environmental Management Science Program, under Contract W-31-109- ENG-38.

DISCLAIMER

Laser Ablation of Concrete

Michael Savina[1], Zhiyue Xu[2], Yong Wang[2], Michael Pellin[1], and Keng Leong[2]

[1]Argonne National Laboratory
Materials Science and Chemistry Divisions
Argonne, Illinois USA

[2]Argonne National Laboratory
Technology Development Division
Argonne, Illinois USA

Abstract

Laser ablation is effective both as an analytical tool and as a means of removing surface coatings. The elemental composition of surfaces can be determined by either mass spectrometry or atomic emission spectroscopy of the atomized effluent. Paint can be removed from aircraft without damage to the underlying aluminum substrate, and environmentally damaged buildings and sculptures can be restored by ablating away deposited grime. A recent application of laser ablation is the removal of radioactive contaminants from the surface and near-surface regions of concrete. We present the results of ablation tests on concrete samples using a high power pulsed Nd:YAG laser with fiber optic beam delivery.

The laser-surface interaction was studied on various model systems consisting of Type I Portland cement with varying amounts of either fine silica or sand in an effort to understand the effect of substrate composition on ablation rates and mechanisms. A sample of non-contaminated concrete from a nuclear power plant was also studied. In addition, cement and concrete samples were doped with non-radioactive isotopes of elements representative of cooling water spills, such as cesium and strontium, and analyzed by laser-desorption mass spectrometry to determine the contamination pathways. These samples were also ablated at high power to determine the efficiency with which surface contaminants are removed and captured.

The results show that the neat cement matrix melts and vaporizes when little or no sand or aggregate is present. Surface flows of liquid material are readily apparent on the ablated surface and the captured aerosol takes the form of glassy beads up to a few tens of microns in diameter. The presence of sand and aggregate particles causes the material to disaggregate on ablation, with intact particles on the millimeter size scale leaving the surface. Laser desorption mass spectrometric analysis showed that cesium and potassium have similar chemical environments in the matrix, as do strontium and calcium.

Introduction

The waste stream generated in the decontamination and decommissioning of nuclear facilities includes a significant volume of material that is contaminated only in the surface or near surface region. Often this material is trapped in lead paint, further complicating disposal problems by making this waste stream a mixed waste. Furthermore, characterization costs associated with shipping test samples off-site are not insignificant. Removal of the contaminated layer would greatly reduce the volume of waste requiring storage. The US Department of Energy and others engaged in the decontamination and decommissioning of nuclear facilities may realize a significant cost benefit if this surface material is analyzed and separated from the uncontaminated bulk material.

These problems can be addressed by a laser ablation system. A high intensity laser beam delivered via a fiber optic cable can ablate contaminated concrete surfaces. The resulting effluent, consisting of aerosol and disaggregated particles, can be efficiently collected with a vacuum shroud and filtration system, and analyzed for contaminants on-line via mass spectrometry or atomic emission spectroscopy. The objectives of this research are to understand the depth-dependent concentration and chemistry of radionuclide-contaminated concrete surfaces, to determine the mechanism and efficacy of laser ablation in removing contaminated surface layers, and to chemically and physically characterize the captured ablation effluent which would become the stored waste. The research concentrated on the effects of ablation on the cement phase of concrete, since this is where the contaminant ions reside.

Experimental

Samples consisted of specimens of non-contaminated high density concrete from the Experimental Boiling Water Reactor at Argonne National Laboratory and samples cast in the laboratory using Type I Portland cement and either fine silica or sand at levels ranging from 0 to 60%. Some samples of concrete and cement were doped with non-radioactive CsCl or $SrCl_2$, to simulate two of the common contaminants, at levels ranging from 10^{-2} to 10^{-6} atom percent.

Laser ablation experiments were done with the 1064 nm fundamental of an Electrox 1.6 kW pulsed Nd:YAG laser. The beam was delivered via a fiber optic cable, focused to a 0.55 mm spot via a 120 mm lens. The typical free-running Nd:YAG pulse energy was 2 J at a pulse length of 0.5 ms and pulse repetition rate of 400 Hz. The sample stage was moved under the stationary beam at a rate of 10 cm/s, giving a pulse overlap of ~50%. Likewise, the groove overlap was ~50%.

The ablated material was captured either on a 0.2 μm Nucleopore filter or with an impactor particle size analyzer. The ablation effluent was analyzed via electron microscopy and energy dispersive X-ray spectroscopy (EDX).

Virgin and ablated surfaces were chemically analyzed with laser desorption / laser photoionization mass spectrometry (LD/PI-MS). Figure 1 is a schematic of the instrument. Samples were introduced to a vacuum chamber at 10^{-9} Torr, where a pulsed laser focused on the surface desorbed a small amount of material, generally less than one atomic layer per pulse. A second pulsed laser focused parallel to the surface at a distance of approximately 0.5 mm above the surface intersected the plume of desorbed material, and ionized a fraction of the atoms and molecules within the focal volume. The ions were accelerated into a 1.2 m drift tube to disperse them according to their mass-to-charge ratio, and detected on a microchannel plate detector.

Results and Discussion

Samples of Type I Portland cement containing 20% of fine (300 μm) silica melted, flowed, and vaporized when ablated with the Nd:YAG laser. Figure 2 is an electron micrograph of several ablation tracks in the material, and shows considerable melting and flow, especially in the region where the laser was slowed to a halt, resulting in many overlapped pulses. The tracks are roughly the same width as the beam, about 0.6 mm, and ~0.5 mm deep. Figure 3 is a high magnification micrograph of the interior of a groove, and shows melting and foaming of the cement matrix, along with a fractured silica grain. In addition, spheres of melted/resolidified cement in sizes ranging from sub-micron to 20 μm are seen in this micrograph. The spheres are also seen in micrographs of the virgin surface, indicating some spatter of the ablated material back onto the surface. Figure 4 is a micrograph of the effluent resulting from the laser ablation of the sample, and shows a range of fine particles in the size range from sub-micron to a few tens of microns. Many of the large spheres have holes or dimples, while the smaller ones appear to be solid. There are also some small irregular chunks of material.

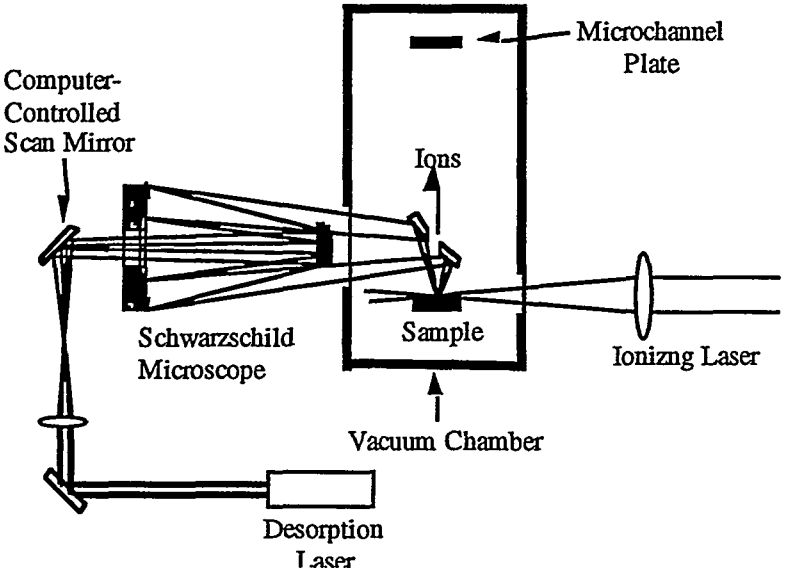

Figure 1: Schematic representation of laser desorption / laser ionization mass spectrometer

The laser-surface interaction in these samples appears to be simple heating, melting, and vaporization. The foamy appearance of the ablated surface is due to the melting and rapid dehydration of the cement. The cement samples typically contained 5% of labile water, and another 20-30% of water of hydration. The rapid release of this water at high temperature results in a steam explosion which propels the bulk of the effluent away from the surface and accounts for the observed structure of both the foamy surface and the hollow spheres. Only the smallest spheres appear to be solid, indicating perhaps that these particles formed from vaporized material. This conclusion is supported by EDX spectra (see below).

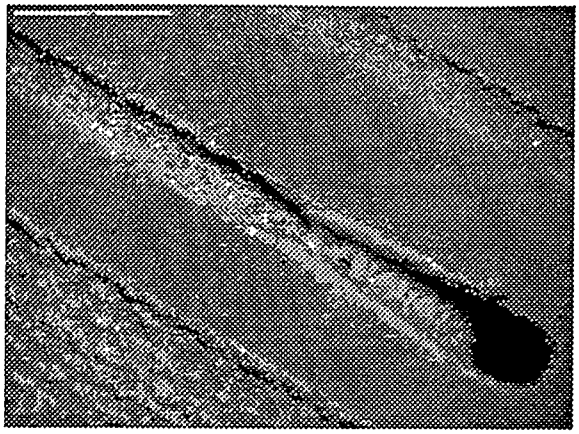

Figure 2: Electron micrograph of ablation grooves in a cement sample containing 20% silica. Bar length is 2 mm.

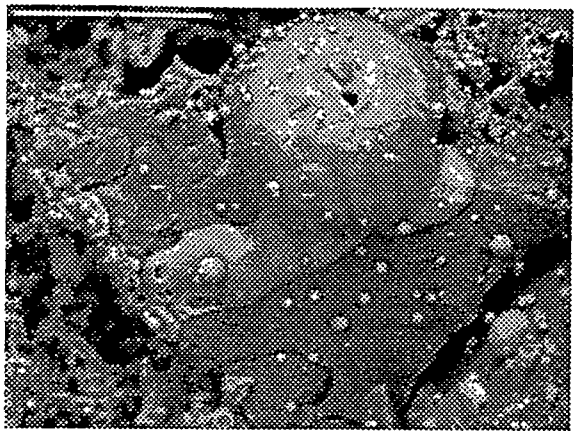

Figure 3: Electron micrograph of an ablated cement surface. Bar length is 50 μm.

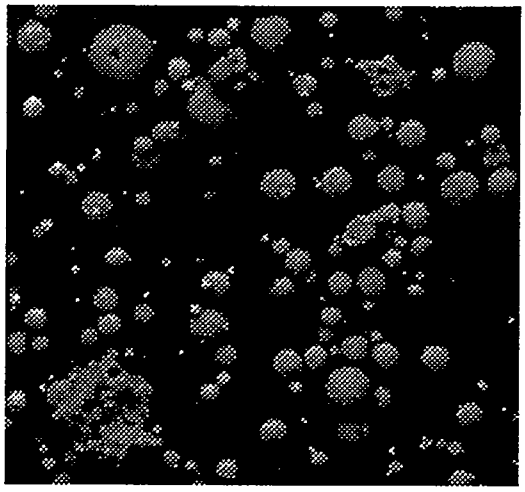

Figure 4: Electron micrograph of the aerosol resulting from the laser ablation of a cement sample containing 20% silica. Field of view is ~150 microns.

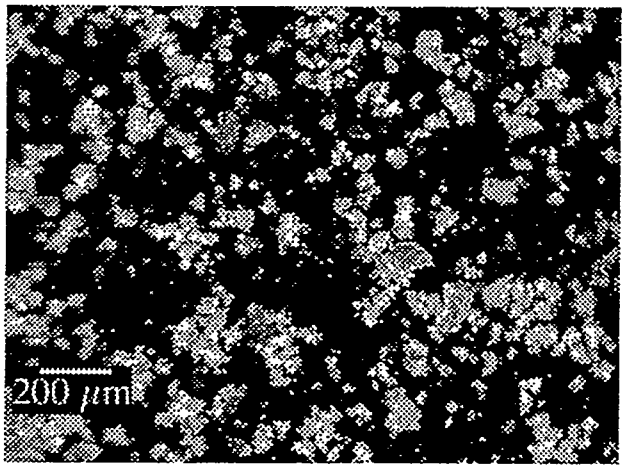

Figure 5: Optical micrograph of fractured and disaggregated material from a cement sample containing 60% sand.

When the filler was changed from 20% fine silica to 20-60% coarse sand (0.5 - 1 mm diameter), the ablation mechanism become more complex. In addition to the fine aerosol particles, a considerable amount of fractured and dislodged material was produced. Figure 5 is an optical micrograph of the effluent from a 60% sand sample showing fractured sand particles and dislodged chunks of cement in a size range up to a few hundred microns. This material was not swept into the impactor system, but was collected from the surface of the sample stage. The impactor collected the fine aerosol as before, along with irregular chunky particles up to 200 μm in diameter. The results indicate that the energy deposited in the sand particles results not in melting, as is the case in the cement matrix, but in rapid heating and thermal shock that fractures the particle. The resulting shock wave fractures and dislodges portions of the cement matrix, resulting in the irregular chunks of material in the effluent observed in Figure 5.

Ablation of high density concrete, which contains sand, aggregates (rocks) ranging up to a few cm in diameter, and very little cement (typically ~10%) produced fractured and dislodged chunks of material up to a ~0.3 mm across, with very little aerosol. The original exterior surface of the high density concrete was simpler than the interior sections, consisting of a 1-2 mm thick layer of Portland cement / sand matrix mostly free of large aggregates, due to settling during casting. This material was ablated with the highest efficiency of any sample tested, with ablation rates up to ten times higher than the fresh Portland cement samples cast in our laboratory (0.4-0.8 mm^3/pulse vs. 0.07 mm^3/pulse). The material disaggregated under the influence of the laser, with particles up to 0.5 mm in diameter dislodged. The difference in ablation behavior may be due either to high sand content in the high density concrete or to the expected presence of $CaCO_3$ in the near-surface region of the sample after many years of exposure to air and/or water[1-3]

EDX spectra of the ablation effluent from the Portland cement samples filled with sand confirmed that both the larger aerosol particles and the chunky material were identical in composition to the virgin cement, while the angular, fractured grains were silica. An interesting trend was noted in the EDX spectra of small solid spheres, however. In general, smaller spheres were richer in aluminum. For example, the aluminum content of 5 μm spheres was 7.5%, while that of 15 μm spheres was 4.6%. The aluminum content of the Type I Portland cement before ablation was 2.5%. This finding supports the conclusion that the small solid spheres are produced by condensation from the vapor phase, and that the nucleating phase is rich in aluminate.

Portland cement is a complex material containing many distinct chemical phases. The principle phases are hydrated calcium silicates, while the second most abundant are hydrated calcium aluminates. Since the EDX technique probes to a depth of ~1 μm, the spectra are showing the near-surface region of the spheres. Therefore, probing smaller and smaller spheres is similar to performing a depth profile of one large sphere. The aluminum concentration rises as one approaches the heart of a sphere, indicating that an alumina or aluminate phase is responsible for nucleation. This finding is significant in light of literature showing that Cs ion binds preferentially to alumina and aluminum-rich phases[4, 5]. Given an EDX detection limit of 1%, the Cs and Sr concentration in our samples was too low to be detected.

LD/PI-MS of the cement samples (Figure 6) showed Mg, Al, Si, and Ca, representative of the cement matrix, and Na and K, representative of the cement pore water and interstitial spaces[6, 7]. The ionizing laser wavelength was 193 nm (ArF excimer), so the spectrum is skewed toward those elements and molecules with ionization potentials below the photon energy of 6.4 eV, including all of those listed above. These species are far more efficiently detected than others, since one-photon ionization is orders of magnitude more efficient than multiphoton ionization. In addition, the spectrum shows a Cs "direct ion," produced by the interaction with the desorbing laser alone. In fact, the direct Cs ion signal outstrips the Cs photoion signal, indicating that cesium, like potassium and other low ionization potential ions, desorbs with a high ion/neutral ratio (the K direct ion is off scale in Figure 7). This is not the case for the other ions in the spectrum. Photoionization is preferable to direct ion mass spectrometry for this application, however, since direct ion spectra suffer from poor reproducibility[8]. Given the signal-to-noise ratio of the Cs photoion peak, we estimate a Cs detection limit of 1-10 ppm for the photoionization spectrum, and somewhat lower for the direct ion spectrum. The Sr detection limit is 1-2 orders of magnitude higher, owing to the fact that Sr does not desorb as easily as Cs (see below).

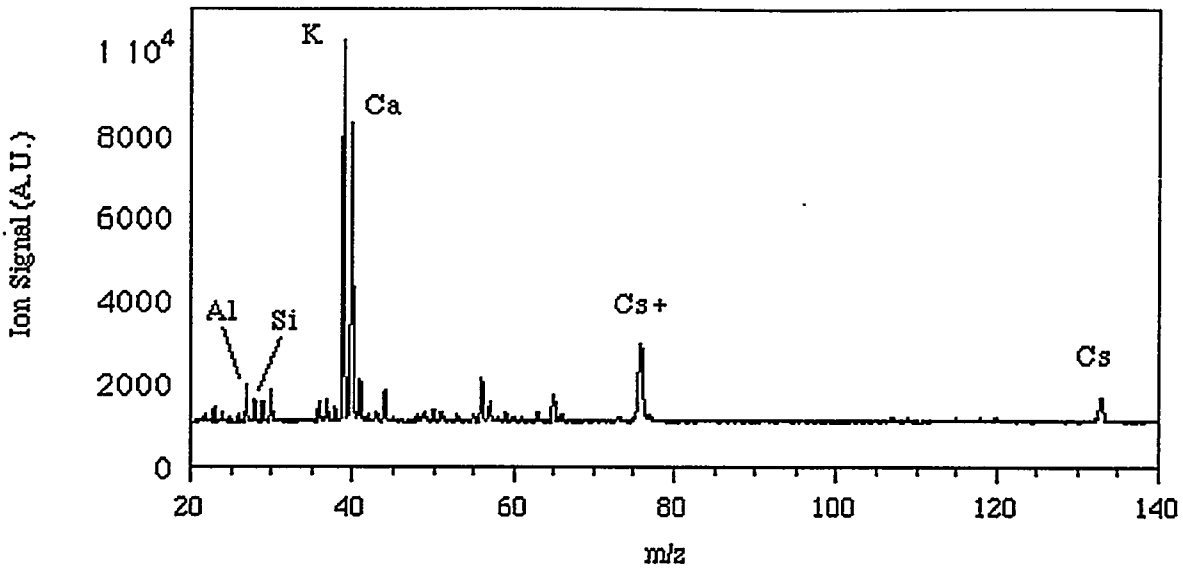

Figure 6: Laser desorption / laser photoionization mass spectrum of a cement smple containing 100 ppm CsCl.

LD/PI-MS also gives some information on the chemical environment of the ions. Ion signals vary from pulse to pulse due in part to fluctuations in the desorbing laser power. If the ionization event is saturated, i.e. if the ion signal does not increase with increasing ionization laser power, then the ion signal becomes a direct measure of the amount of material desorbed. This does not hold for non-resonant multiphoton ionization schemes, which are rarely saturated, however the one-photon scheme employed here is saturated. One can then probe the desorption dynamics of the various ions of interest using the natural power fluctuations of the desorbing laser. The Cs and K photoion signals are large compared to the Ca photoion signal even though Ca is at least three orders of magnitude more abundant in the material. This is due in large part to the fact that Cs and K are far easier to desorb than Ca. The absolute pulse-to-pulse variation in Cs and K signals is also much greater than that of the Ca signal, however the standard deviation of the ion signal as a fraction of the mean of many pulses is lower for Cs and K than for Ca and Sr.

Table 1 gives the means and standard deviations for K, Ca, Cs, and Sr. It shows that K and Cs desorb very similarly, and thus have similar chemical environments, while the same is true for Ca and Sr. Cesium therefore probably resides in the cement interstitial pore water as does potassium[6, 7], while strontium is a part of the cement matrix as is calcium. This is to be expected owing to the chemical similarities between Cs and K and between Sr and Ca.

Sample	Ion	Std. dev. / mean
1	K	0.67
1	Ca	1.22
1	Cs	0.73
2	K	0.22
2	Ca	0.67
2	Sr	0.61

Table 1: Standard deviations as a fraction of the mean of ion signals from cement samples doped with (1) CsCl and (2) $SrCl_2$. One thousand shots were averaged for each sample. The differences in the values for the same ions across the two samples are due to absolute differences in the desorbing laser intensity.

Conclusions

Laser ablation of cement and concrete produces greatly varying effluents and ablation rates depending on the age and composition of the material. The cement matrix itself melts, dehydrates, and vaporizes when ablated with a high-power pulsed Nd:YAG laser, while sand and aggregate material tends to fracture and dislodge without melting. The aerosol produced from the cement matrix consists of particles similar in chemical composition to the original cement, with the exception that the smaller aerosol particles tend to be enriched in aluminum, owing to nucleation by an alumina or aluminate phase. Laser desorption mass spectrometry shows that Cs can detected at the ppm level, and that Cs and K share similar chemical environments, as do Sr and Ca.

This work was supported by the U.S. Department of Energy, BES-Materials Science, under Contract W-31-109-ENG-38; and by the U.S. Department of Energy, Environmental Management Science Program, under Contract W-31-109-ENG-38.

References

1. Cowie, J., and Glasser, F. P. "The reaction between cement and natural waters containing dissolved carbon dioxide." *Adv. Cem. Res.*, 4: (1992) pp. 119-1 Structures and Decomposition of C-S-H." *Cem. Concr. Res.*, 24: (1994) pp. 55-61.
3. Sarott, F. A., Bradbury, M. H., Pandolfo, P., and Spieler, P. "Diffusion and adsorption studies on hardened cement paste and the effect of carbonation on diffusion rates." *Cem. Concr. Res.*, 22: (1992) pp. 439-444.
4. Groenewold, G. S., Ingram, J. C., McLing, T., Gianotto, A. K., and Avci, R. "Cs+ Speciation on Soil Particles by TOF-SIMS Imaging." *Anal. Chem.*, 70: (1998) pp. 534-539.
5. Hoyle, S. L., and Grutzeck, M. W. "Incorporation of cesium by hydrating calcium aluminosilicates." *J. Am. Ceram. Soc.*, 72: (1989) pp. 1938-1947.
6. Angus, M. J., and Glasser, F. P. "The chemical environment in cement matrixes." *Mater. Res. Soc. Symp. Proc.*, 50: (1986) pp. 547-556.
7. Berner, U. R. "Modeling porewater chemistry in hydrated portland cement." *Mater. Res. Soc. Symp. Proc.*, 84: (1987) pp. 319-330.
8. Savina, M. R., and Lykke, K. L. "Microscopic Chemical imaging with Laser Desorption Mass Spectrometry." *Anal. Chem.*, 69: (1997) pp. 3741-3746.